Towards Optimized Actuation for Legged Robots—Ideal Gear Ratios for a 2 Degree-of-Freedom Jumping Leg.

Adi Mehrotra
Department of EECS, MIT
MIT Biomimetic Robotics Lab
Cambridge, USA
adim@mit.edu

Fiona Gillespie
Department of EECS, MIT
MIT Sea Grant Lab
Cambridge, USA
fgillesp@mit.edu

***Abstract*—Optimized actuation for legged robots is a complex problem involving interactions between the motor's electromagnetic parameters, reflected inertia through the gearbox, and stiction [1]. This paper begins to explore optimized actuation for dynamic legged robots by considering only inertia and both a 1DoF and 2DoF simplified leg model to find the optimal gear ratio for jumping. A simple direct collocation trajectory optimization was used to create max jump height trajectories using MATLAB and CasADi [2]. We present a more precise approach to modeling motor torque-speed curve constraints in the optimization than the traditional actuation "box" constraints. Motor and leg parameters were held constant while the outer loop iterated over gear ratios selecting the ratios that produced the maximum jumping height. We found an optimal gear ratio of 10.5 at the hip actuator for the 1DoF leg and optimal gear ratios of 9.5 at both the hip and knee for the 2DoF case. We end with a discussion on future work involving modeling friction, and changing leg and motor parameters to determine their effects on the optimal gear ratio.**

***Index Terms*—robotics, trajectory optimization, motors, gear ratios, co-design**

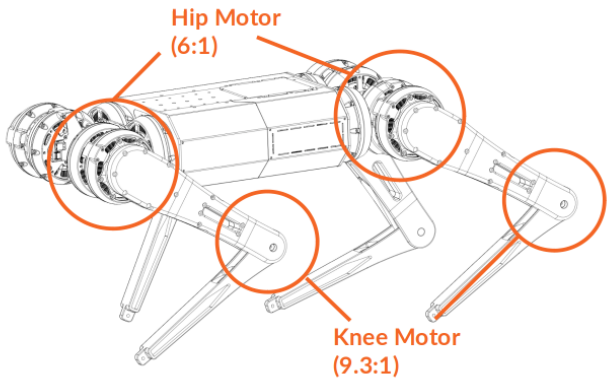

Fig. 1. The original Mini Cheetah has a 6:1 gear ratio at the hip and a 9.3:1 gear ratio at the knee. We want to know if we can optimize these gear ratios for the specific task of jumping.

I. Introduction

The topic of optimized actuation for legged robots has been a research interest for some time now. Legged robot actuation is specific in its need in that actuators must be able to produce large amounts of power and torque while also being robust to impacts with the environment [3]. The ANYmal robot solved this by using a high gear reduction harmonic drive connected to a brushless motor with a torque-sensing spring on the output shaft, this paradigm is called Series-Elastic actuation (SEA) [4]. The MIT Cheetah and Mini Cheetah platforms used a combination of high torque density motors and low gear ratios to minimize inertia using the motor itself to measure torque output: this paradigm is called Proprioceptive actuation [5] [6]. A review of these actuation paradigms and considerations for actuation for legged robots is presented in [3].

However, these works present general approaches to actuation that we have started calling "actuation paradigms" as noted earlier. They do not look at further optimizing these parameters to produce certain behaviors on the robot. This "co-design" is a newer trend. Work from [1] uses a nonlinear optimization to narrow down a motor-gearbox pair choice for the task of jumping. And work from [7] presented metrics for motor selection independent of gear ratio. We hope to combine both of these in future work as a guide for optimized actuator design for legged robots.

This paper focuses most on initially replicating work from [1]. Replicating work from previous papers is the first step towards extending it in the future. We modeled a 1DoF jumping leg in MATLAB and created an optimization for maximum jump height using CasADi [2]. We then searched over gear ratios finding the optimal gear ratio for 1DoF jumping for the Mini Cheetah leg was 10.5 at the hip and the leg performed classic bang-bang control. We then extended this to the 2DoF case and found that the optimal gear ratios were equal between the hip and the knee (with the most optimal gear ratio being 9.5), and the leg still performed classic bang-bang control. This result was different than what we expected and warrants future work which we discuss in the last sections of this paper.

MIT Biomimetic Robotics Lab, MIT Department of Mechanical Engineering, MIT EECS

II. Problem Setup

A. Motor Torque-Speed Curves

We start with a short discussion on motor torque-speed curves for those who are not familiar. A motor's performance characteristics are defined by its torque-speed curve. As an electro-mechanical transducer, a motor has hard performance limits defined by physics and these are presented in the form of a torque-speed curve. The limits on a motor's performance are complicated but can be approximated into three constraints, which are found through motor testing [8] and presented in Figure 2. We present the process of simplifying a real torque-speed curve into this lower order model in section III.B.

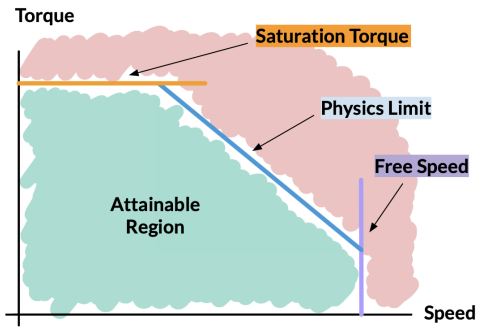

Fig. 2. A simplified diagram of a typical motor torque-speed curve with the attainable and unattainable regions, as well as the limit lines labeled.

The first constraint (the horizontal orange line) represents the maximum torque the motor can produce due to magnetic saturation of the stator core. Since torque is produced by magnetic field interactions, when the stator core reaches saturation no more torque can be produced. The second constraint (the vertical purple line) represents the free-speed of the motor or the maximum speed the motor can spin under no load. This comes from an interaction between the applied voltage and the back-EMF produced by the motor. The third limit (the diagonal blue line) comes from a complex set of interactions including the motor winding resistance, inductance, power limits, thermal properties, and etc. But it can be simply approximated as a limit on the torque as a linear function of the speed of the motor [9].

Gear ratios affect a motor module by shifting these constraints. Increasing the gear ratio will increase the saturation torque, and decrease the free-speed. The limit line will shift according to Figure 3.

Further discussion of torque-speed curves, motor testing, motor parameters, and performance characteristics are presented in previous work and is linked here for educational purposes [8].

B. Defining the Problem

We decided to optimize the peak jump height for a simplified model of the Mini Cheetah robot as presented in [6]. Figure 4 displays a sketch of the Mini Cheetah jumping where

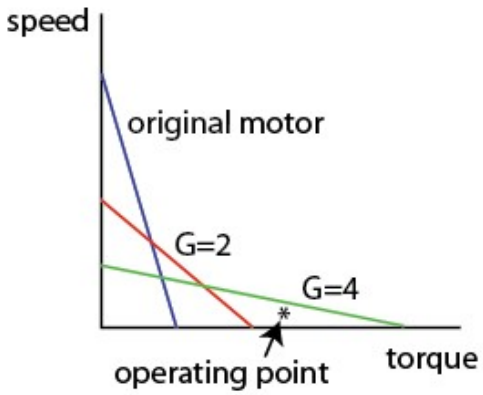

Fig. 3. Gear ratio affect on torque-speed curve limit line as presented in [10]. NOTE that the axis for torque and speed are flipped in this figure as compared to Figure 2 (we apologize).

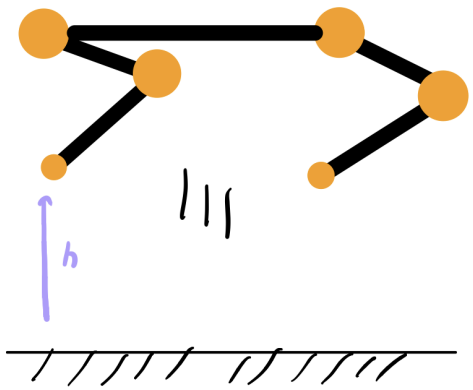

Fig. 4. Diagram of simplified 2D mini cheetah jump, where h represents the height

the height is defined as the height of the foot above the ground at the peak of the trajectory.

The problem of jumping was chosen because it has a non-trivial solution based on the true constraints of a torque-speed curve. Most optimizations only account for the saturation torque and the free-speed of the motor, modeling the constraint as a "box" of possible actuation efforts in the torque/speed plane shown in Figure 5. We present a more accurate modeling which includes the physical limit line in our optimization. This is shown in Figure 6.

In this case jumping has a "nontrivial solution" because the highest gear ratio would not allow the Mini Cheetah to jump the highest because of the trade-off with speed of the motor, while the lowest gear ratio would not have enough torque to lift the leg. There is a middle ground here that is difficult to mathematically define but intuitively easy to understand. The optimizer should attempt to find the gear ratio that provides enough torque but does not limit the maximum velocity of the foot at takeoff.

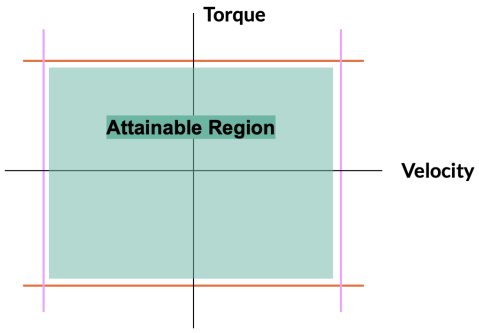

Fig. 5. Box constraints on the actuation efforts.

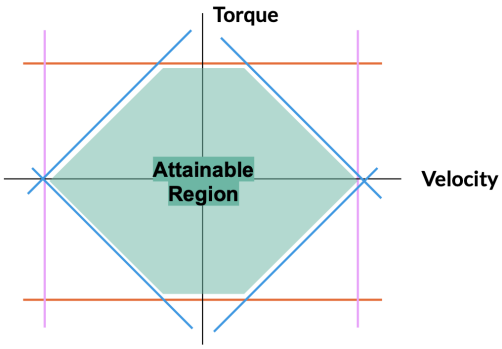

Fig. 6. More accurate constraints including the limit lines.

III. Approach

A. Modeling

The full 3D Mini Cheetah is rather complex, so we started with a simple one degree of freedom "uniroo" style model. Figure 7 shows this modeling with 2 state variables: y and θ. y represents the height of the foot above of the ground and θ represents the angle between the horizontal and the knee joint. For simplicity, the foot is constrained to stay vertically under the hip, which constrains both joint angles to be equal.

In the two degree of freedom case, Figure 8 shows the 3 state variables: y, θ_1, and θ_2. y again represents the height of the foot. Now θ_1 represents the angle between the horizontal and the hip joint, and θ_2 the angle between the horizontal and the knee joint. The angles were defined with respect to the horizontal for geometric simplicity.

B. Motors

For the motor and gearbox modeling we started with a model of the T-Motor U8 which was used in the original Mini Cheetah as presented in [11]. The torque-speed curve of just the motor with no gearbox is shown in Figure 9. As described in the previous section we can approximate this curve using three constraints.

The first two constraints are the saturation torque which we can read off this graph to be around 2.7 $\mathrm{N\,m}$ and the free-speed

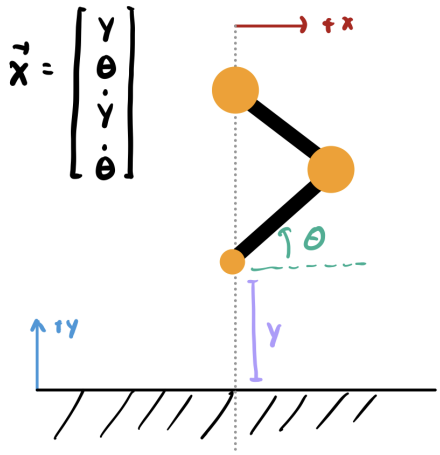

Fig. 7. One Degree of Freedom Leg Model

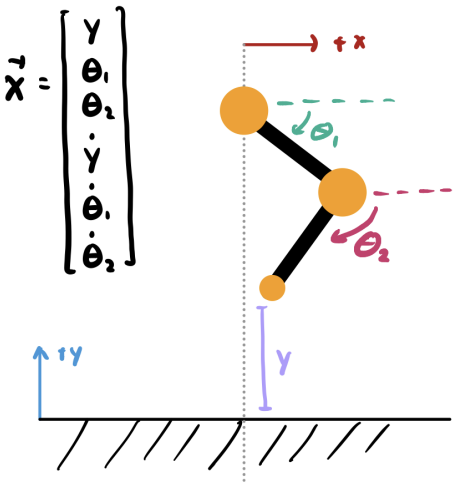

Fig. 8. Two Degree of Freedom Leg Model

which is around 190 $\mathrm{rads/s}$. If we account for an arbitrary gear ratio g, this constraint becomes the following.

$$-g \cdot 2.7\mathrm{N\,m} <= T_i <= g \cdot 2.7\mathrm{N\,m}$$

$$-190\mathrm{N\,m}/g <= V_i <= 190\mathrm{N\,m}/g$$

where T_i is the torque at time-step i of the optimization and V_i is the speed at time-step i of the optimization. We can then fit a line of the form $T_i = m \cdot V_i + b$ to the limit line as described in II.A, where m is the slope and b is the y-intercept of the graph. The effect of gear ratio on the line as determined by [10] is shown in the following equation.

$$T_i <= g^2 \cdot m \cdot V_i + b \cdot g$$

We add the $<=$ constraint because the torque-speed point (or the actuation point) may lie under or on the limit line but never above. Also note that the effect on the parameters of

this fitted line is not linear. The m value increases with g^2 while b only increases linearly with g.

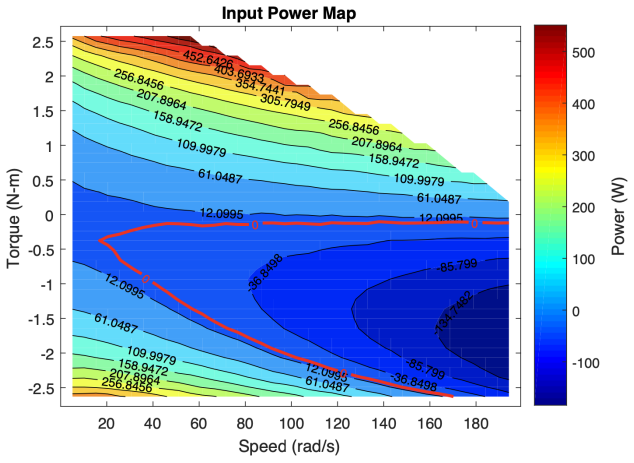

Fig. 9. Motor testing data from the original U8 module from [11].

C. Structure

We iterated over a range of gear ratios for both the hip and knee actuators. For each iteration, we used trajectory optimization to apply actuation during the stance phase, and use the optimal states and inputs found to simulate what the peak height would be through projectile motion. The height is recorded for each gear ratio combination, and the full results are visualized in a later section.

In the following subsection we will discuss the full trajectory optimization problem.

D. Trajectory Optimization

At a high-level, our optimization maximizes the peak height of the jump, with the traditional dynamics and boundary constraints, and our actuator constraint approximations. We used the CasADi library for MATLAB with the Ipopt solver to perform our optimization [2].

Now we will introduce some key parameters and then explain the full formulation.

Key Parameters:

g_1 = hip gear ratio
g_2 = knee gear ratio
T = motor stall torque
S = motor free-speed
m = torque-speed curve slope
b = torque-speed curve intercept
N = timesteps during stance

Here is our trajectory optimization formulation. The following constraints are applied to both gear ratios, but are listed just once for simplicity ($g = g_1, g_2$).

$$\max_{x[\cdot],u[\cdot]} \quad h$$

subject to

1. $h = p(x,u)$
2. $x[n+1] = x[n] + f(x,u)$
3. $y[n] = 0$
4. $F[n] > 0$
5. $-T \cdot g <= u[n] <= T \cdot g$
6. $-V \cdot g <= \dot{\theta}[n] <= V \cdot g$
7. $u[n] - m \cdot \theta[n] <= b$
8. $y[n] + l \cdot \sin(\theta[n]) >= 0$
9. $y[0] = 0, \theta_1 = 60°, \theta_2 = 120°$
10. $\dot{y} = 0, \dot{\theta_1} = 0, \dot{\theta_2} = 0$

The first four constraints involve typical physical and dynamic constraints. The first constraint relates our peak height, h, to the states and inputs through projectile motion, represented by $p(x,u)$. The second constraint enforces the dynamics. The third constraint enforces that the foot is on the ground during the stance phase. The fourth constraint enforces that the ground reaction force, F, cannot pull on the foot, as in there is no stickiness between the foot and the ground.

We would like to highlight constraints 5-7, which represent our approximation of actuator constraints. Constraint 5 provides the torque saturation limit on the input, constraint 6 provides the free-speed limit on the velocity of the leg, and constraint 7 provides the physics motor limit. Together, these constraints force the input to be physically feasible for the motor.

The final three constraints are also typical physical and boundary conditions. The eighth constraint enforces that the leg is above the ground during stance. (In the expanded version, this is applied to both joints. At first we only applied the above ground constraint to the knee joint, and the optimizer had the hip swing below the ground for an extra boost). The ninth and tenth constraints enforce the initial conditions on the positions and velocities of the leg.

Now that we have finished setting up the problem and approach, we will move to a discussion of our results and key findings.

IV. Results

A. One Degree of Freedom

We began with our one degree of freedom leg (1DoF) to verify that our trajectory optimization was well formulated. Figure 10 shows our analysis over gear ratios from 0 to 40, with a step size of 1.

We found the optimal gear ratio to be 10.5, and looked at its torque-speed optimal actuation, as shown in Figure 11. The tan shading represents the motor operation region, and the blue shading shows the unattainable region. The trajectory of torques and speeds is shown as a gradient of pink-to-green as it moves through time. The trajectory of torques and speeds

lies on the boundary of the motor operation region. This shows that the optimizer followed bang-bang control, as expected.

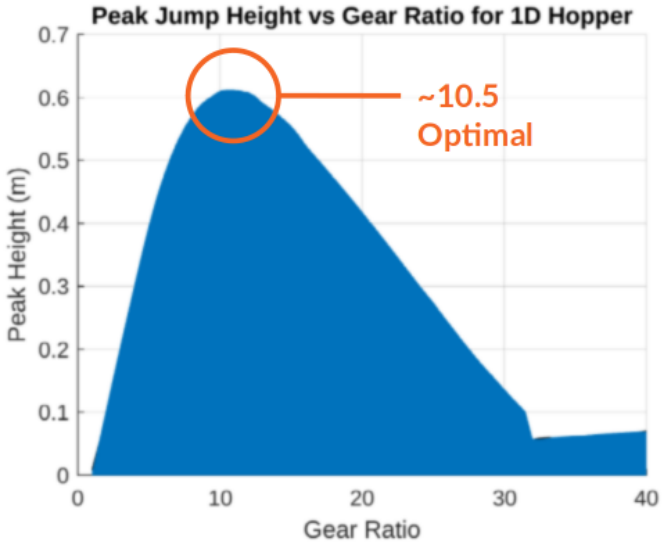

Fig. 10. Area Plot of Height vs Gear Ratio in One Degree of Freedom. Optimal Gear Ratio is 10.5

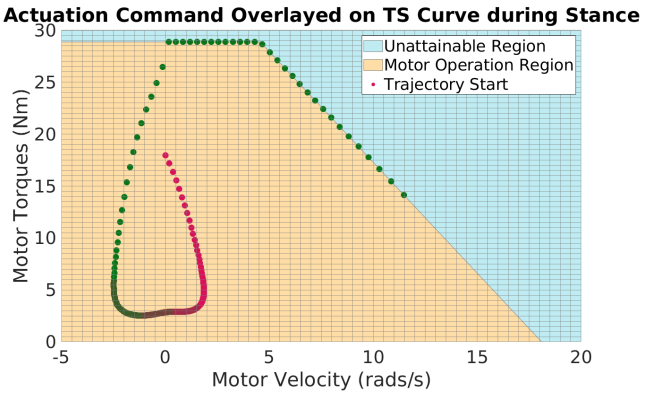

Fig. 11. Torque Speed Curve for One Degree of Freedom. The pink-to-green gradient shows the progression of time. The optimizer follows Bang-Bang control.

B. *Two Degrees of Freedom*

Since the two degree of freedom (2DoF) space is much larger, we began with a coarse search over gear ratios in the range 1:30 with a step size of 2. Figure 12 shows a surface plot of the maximum jump height as a function of the hip gear ratio and knee gear ratio. Figure 13 shows this same analysis as a level set, where the lower heights are closer to purple and the higher heights are closer to yellow. A interesting insight from this analysis was learning that the gear ratios vs height plot was rather symmetric across the line of equal gear ratios. This symmetry is shown by the black dotted line in Figure 13.

Once we found the optimal gear ratio from the coarse search to be 9 for both hip and knee, we performed a finer analysis over the range of 7 to 15 with a step size of 0.5, as seen in

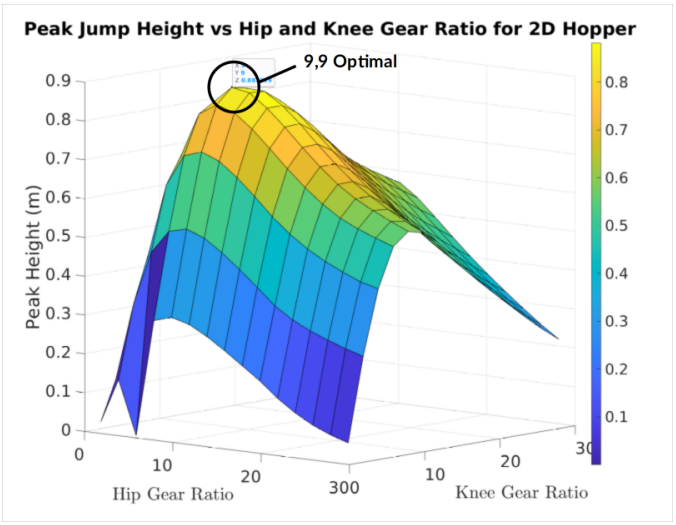

Fig. 12. Surface Plot of Height vs Gear Ratios in Two Degree of Freedom (Step size = 2). Optimal Gear Ratio was 9 for both hip and knee joints

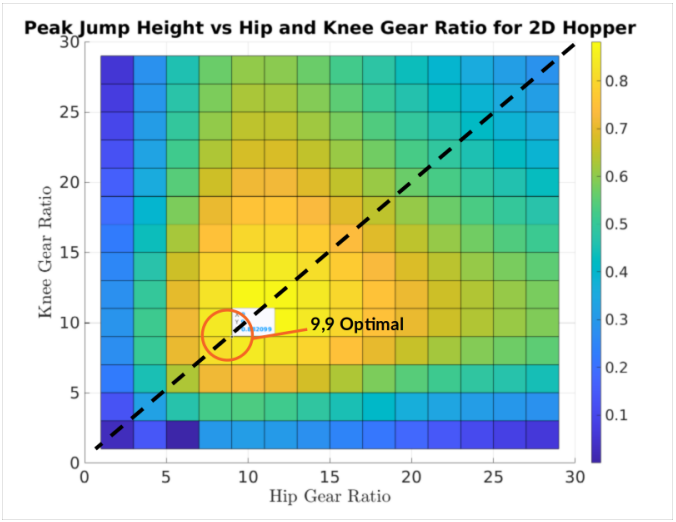

Fig. 13. Level Set Plot of Height vs Gear Ratios in Two Degree of Freedom (Step size = 2). Optimal gear ratio was 9 for both hip and knee. Black dotted line is a line of symmetry with equal gear ratios.

Figure 14. This resulted in the final optimal ratios of 9.5 for both the hip and knee joints.

With the optimal 2D gear ratio of 9.5 for both hip and knee joints, we again plotted a torque-speed curve, shown in Figure 15. In the torque-speed curve, the pink-to-green gradient represents hip actuation over time and the blue-to-black gradient represents knee actuation over time. The optimizer almost exactly matched the actuation for both joints and used bang-bang control, which is interesting and not what we expected.

C. *Interesting Optimization Results*

There was an interesting technique the optimizer used to try to maximize jump height for certain combinations of gear ratios. For example, the gear ratio of 11 at the hip and 6 at

Fig. 14. Surface Plot of Height vs Gear Ratios in Two Degree of Freedom (Step size = 0.5)

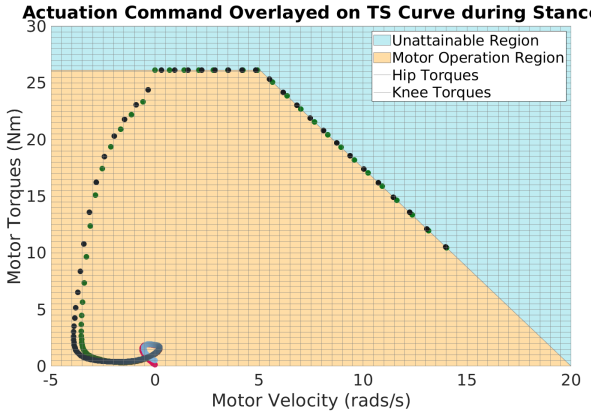

Fig. 15. Surface Plot of Height vs Gear Ratios in Two Degree of Freedom (Step size = 0.5)

the knee produced a "double-jump" effect which is shown in Figure 16.

Around t=1.15s in the optimization the ground reaction force (GRF) goes to zero indicating the foot is about to leave the ground. In response to this, at the next time-step, the optimizer commands full negative torque to the hip joint to place the foot back on the ground and then goes back to commanding positive torque to make the leg jump even higher.

It's important to note that depending on how quickly the motor switches torque and velocity directions this behavior may not be attainable on physical hardware as the amount of regenerative braking power this would produce is extremely high [12]. However, it is interesting to note the solution the optimizer found because it is a creative way to maximize jump height that we did not initially think of. The use of these results on real hardware in the future may not be significant especially because this behavior was not observed at the optimal gear ratio for this specific system, but future work could explore this concept more which could lead to better understanding of the gear ratio's effect on the dynamic performance of a robotic system.

D. Unusual Optimization Results

We also found a few unusual optimization results that warrant future study. A gear ratio of 11 at the hip and 8.5 at the knee resulted in a failure to jump, which was a unique abnormality when searching over the 7-15 ratio range at a 0.5 step size. Visualizing this trajectory showed the foot slipping across the floor. This is shown in Figure 17.

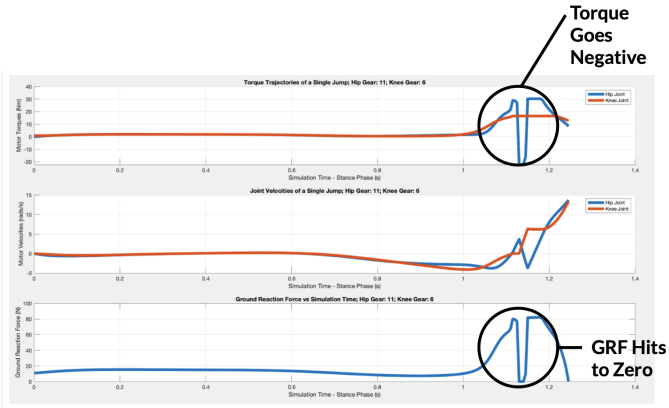

Fig. 16. For a hip gear ratio of 11 and knee gear ratio of 6 the optimizer found a "double jump" solution to make the leg jump higher.

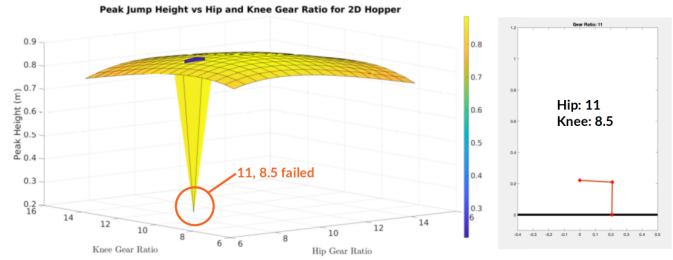

Fig. 17. For a hip gear ratio of 11 and knee gear ratio of 8.5, the hopper was unable to jump. This was unique to this gear ratio combination, and was not seen in the immediately surrounding points.

Initially we thought this could be a simulation error so we performed a finer search in the 8.4-8.6 range with a 0.05 step size on the knee joint and a range of 10.5-11.5 with a step size of 0.05 at the hip joint. The results of this are shown in Figure 18. This produced equally confusing results where some points produced these failed jumps while others jumped normally.

We predict this issue comes from the lack of friction modeling or modeling of any horizontal forces in the optimization. The lack of simple friction constraints could cause strange behaviors in the optimization so including friction could be a good first step to understanding where this behavior is coming from. This behavior is important to understand because it could be indicative of modeling errors or other unknown effects of the gear ratios and inertial parameters on the dynamics of the system.

V. Conclusion

A. Key Findings

Trajectory optimization on a simplified model of a Mini Cheetah leg produced an optimal gear ratio of 10.5 for a 1DoF

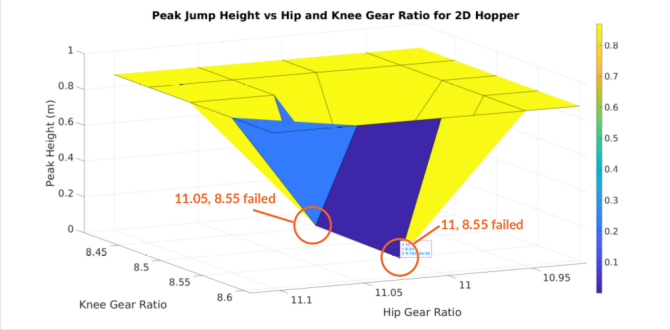

Fig. 18. Searching around the point of failure at a step-size of 0.05 on gear ratios. This produced equally strange results, where hip-knee combinations of (11, 8.5), (11, 8.55), and (11.05, 8.55) failed, but all other combinations in this region jumped normally.

jumping leg and 9.5 for both the hip and the knee joints for the 2DoF jumping leg. For the purposes of our work it's not so much the actual value of the gear ratio we're interested in right now rather than the fact that we now have a framework to determine optimal gear ratios based on a desired task for a legged robotic system.

We also discovered interesting trends, such as the optimal gear ratios for the 2DoF case were equal for the hip and the knee and the surface plot of peak jump height vs hip and knee gear ratios was symmetric about the equal ratios line as described in section IV.B and shown in Figure 13. These trends provide a starting point for future exploration as discussed in the last section of this paper.

Finally, this project taught us a lot about general trajectory optimization, modeling, and constraints, which were areas we had little experience in. It yielded interesting results and produced many avenues for future work that we will describe in the final section.

B. Future Work

This project mainly opened up possibilities for future work in this area. The first area of investigation comes from the fact that the optimal gear ratios for the 2DoF case were equal between the hip and the knee joints and the controller found bang-bang control. This symmetry was surprising at first, but in our simple model, the thigh and shank lengths were equal, and their inertias were rather similar as well. This may have caused the symmetry in the gear ratios we saw. We think an exploration involving varying leg parameters, lengths, and inertias, could allow us to determine the leg parameters' effects on the value of the optimal gear ratios. It would be mainly interesting to see what leg produces gear ratios that are different between the hip and the knee and if that produces a controller different from bang-bang control.

Our simplified model also did not take into account impact or contact. Impact is a significant consideration when designing gear ratios as if the reflected inertia and the effective mass is too high, this can produce an impulse during landing so large that the sun gear inside the robot's planetary gearbox could fail. The next step would be to model this impulse and the failure torque of the module to see if the leg is violating that constraint or if that changes the output of the optimization.

We also discussed some unusual optimization results in section IV.D which included much lower jump heights or even failure to jump in the area of ratio 11 for the hip and 8.5 for the knee. This was an interesting and surprising result and we think it may have to do with the fact that the model doesn't currently model any x-forces or friction. We think an accurate model of friction is a good first step to understanding what may be causing the issues around this area. These issues could also provide insight into actuator parameter's effects on the dynamics of a robot.

Finally our model could be expanded to include more complexity. Since we had many constraints, we chose to use one leg and only maximize height. In the future, costs on actuation could be explored and the modeling could extend to the 2D or 3D case. We could also look at papers such as [13] which include modeling the effects of the actuator in the actual dynamics equations of the robot. We could also expand the actuator model to include more details such as those presented in [1] and [7].

Overall we are excited for the future possibilities of our work in using computation as a design tool for optimal actuation for legged robotic systems.

VI. Acknowledgement

The authors would like to thank Professor Russ Tedrake, Alexandre Amice, Lujie Yang, and the 6.832 Underactuated Robotics course staff for a great semester! We would also like to thank Matt Chignoli and Charles Khazoom for all the help with trajectory optimization and creating simple tutorials for us to follow. We'd like to thank Fischer Moseley for his late night debugging help and for being a very sturdy wall to bounce ideas off of. Finally, we'd like to thank Elijah B. Stanger-Jones, Steve Heim, and Andrew SaLoutos for their help in formulating this research project.

VII. Team Member Contributions

The work was split fairly evenly. Adi focused mostly on developing the robot model and actuator model figuring out how to accurately model those in simulation. Fiona mostly focused on formulating the trajectory optimization and collecting results. Both authors worked together on analysis and interpretation as well extending the current results to future work.

VIII. Links to Code and Video

A video associated with this paper can be found here.

The MATLAB code associated with this paper is linked in this GitHub repo. Users will need to install CasADi.

References

[1] Y. Ding and H.-W. Park, "Design and experimental implementation of a quasi-direct-drive leg for optimized jumping," in *2017 IEEE/RSJ International Conference on Intelligent Robots and Systems (IROS)*, 2017, pp. 300–305. DOI: 10.1109/IROS.2017.8202172.

[2] J. A. E. Andersson, J. Gillis, G. Horn, J. B. Rawlings, and M. Diehl, "CasADi – A software framework for nonlinear optimization and optimal control," *Mathematical Programming Computation*, vol. 11, no. 1, pp. 1–36, 2019. DOI: 10.1007/s12532-018-0139-4.

[3] P. M. Wensing, A. Wang, S. Seok, D. Otten, J. Lang, and S. Kim, "Proprioceptive actuator design in the mit cheetah: Impact mitigation and high-bandwidth physical interaction for dynamic legged robots," *IEEE Transactions on Robotics*, vol. 33, no. 3, pp. 509–522, 2017. DOI: 10.1109/TRO.2016.2640183.

[4] M. Hutter, C. Gehring, D. Jud, *et al.*, "Anymal - a highly mobile and dynamic quadrupedal robot," in *2016 IEEE/RSJ International Conference on Intelligent Robots and Systems (IROS)*, 2016, pp. 38–44. DOI: 10.1109/IROS.2016.7758092.

[5] G. Bledt, M. J. Powell, B. Katz, J. Di Carlo, P. M. Wensing, and S. Kim, "Mit cheetah 3: Design and control of a robust, dynamic quadruped robot," in *2018 IEEE/RSJ International Conference on Intelligent Robots and Systems (IROS)*, 2018, pp. 2245–2252. DOI: 10.1109/IROS.2018.8593885.

[6] B. Katz, J. D. Carlo, and S. Kim, "Mini cheetah: A platform for pushing the limits of dynamic quadruped control," in *2019 International Conference on Robotics and Automation (ICRA)*, 2019, pp. 6295–6301. DOI: 10.1109/ICRA.2019.8793865.

[7] K. Urs, C. E. Adu, E. J. Rouse, and T. Y. Moore, *Alternative metrics to select motors for quasi-direct drive actuators*, 2022. arXiv: 2202.12365 [cs.RO].

[8] A. Mehrotra, *Dynos for Dummies (And other interesting motor things...)* Department of Alchemy, 2022. eprint: https://www.adim.io/_files/ugd/067a81_c7165eb397794bbf8eab9d27706da229.pdf.

[9] S.-H. Kim, *Electric Motor Control - DC, AC, and BLDC Motors*. Elsevier Science, 2017.

[10] *Choosing a Motor and Gearing Combination*. Northwestern Center for Robotics and Bio Systems. eprint: http://hades.mech.northwestern.edu/index.php/Choosing_a_Motor_and_Gearing_Combination.

[11] B. Katz, *A low cost modular actuator for dynamic robots*. Department of Mechanical Engineering, MIT, 2018.

[12] E. B. Stanger-Jones, *Expanding the Capabilities of Dynamic Robotic Systems*. Department of Electrical Engineering and Computer Science, MIT, 2022.

[13] Y. Sim and J. Ramos, "The dynamic effect of mechanical losses of actuators on the equations of motion of legged robots," *CoRR*, vol. abs/2011.02506, 2020. arXiv: 2011.02506. [Online]. Available: https://arxiv.org/abs/2011.02506.